Science Advances
AAAS

Supplementary Materials for

Identification of an ionic mechanism for ERα-mediated rapid excitation in neurons

Meng Yu *et al.*

Corresponding author: Yong Xu, yongx@bcm.edu; Yanlin He, yanlin.he@pbrc.edu

Sci. Adv. **10**, eadp0696 (2024)
DOI: 10.1126/sciadv.adp0696

The PDF file includes:

Other Supplementary Material for this manuscript includes the following:

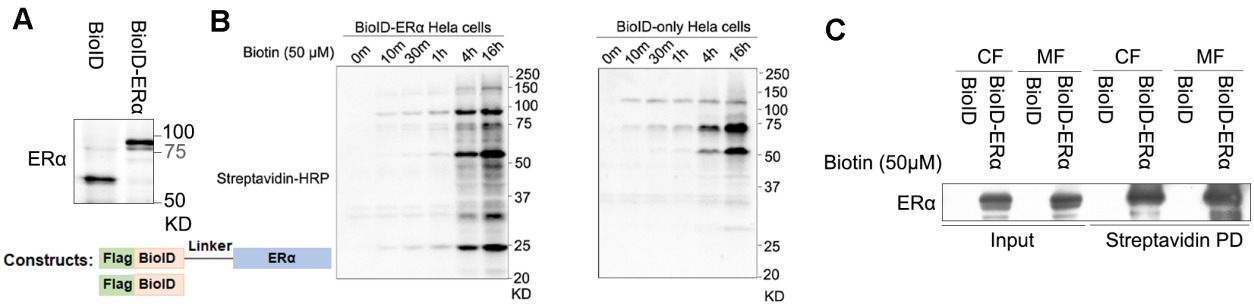

Figure S1. BioID to identify ERα-interacting proteins. (A) Validation of stable Hela cell lines expressing BioID-ERα (or BioID only). Hela cells expressing BioID-ERα (or BioID only) were harvested and lysed. Western blotting was employed to determine ERα expression in the stable cells with ERα antibody. (B) In vitro biotinylation at variable biotin treatment time. Hela cells expressing BioID-ERα (or BioID only) were treated with 50 μM biotin for variable time. Biotinylation levels were determined by Western blotting with an HRP-conjugated streptavidin antibody. (C) Streptavidin pulling down biotinylated proteins in Hela cell lines expressing BioID-ERα (or BioID only). Biotin was administered to stable Hela cells for 16 hours, and subsequent separation of cytoplasmic and membrane fractions was performed. Biotinylated proteins in the subcellular fractions were affinity purified using streptavidin magnetic beads. ERα expression in the pull-down samples was assessed by Western blotting.

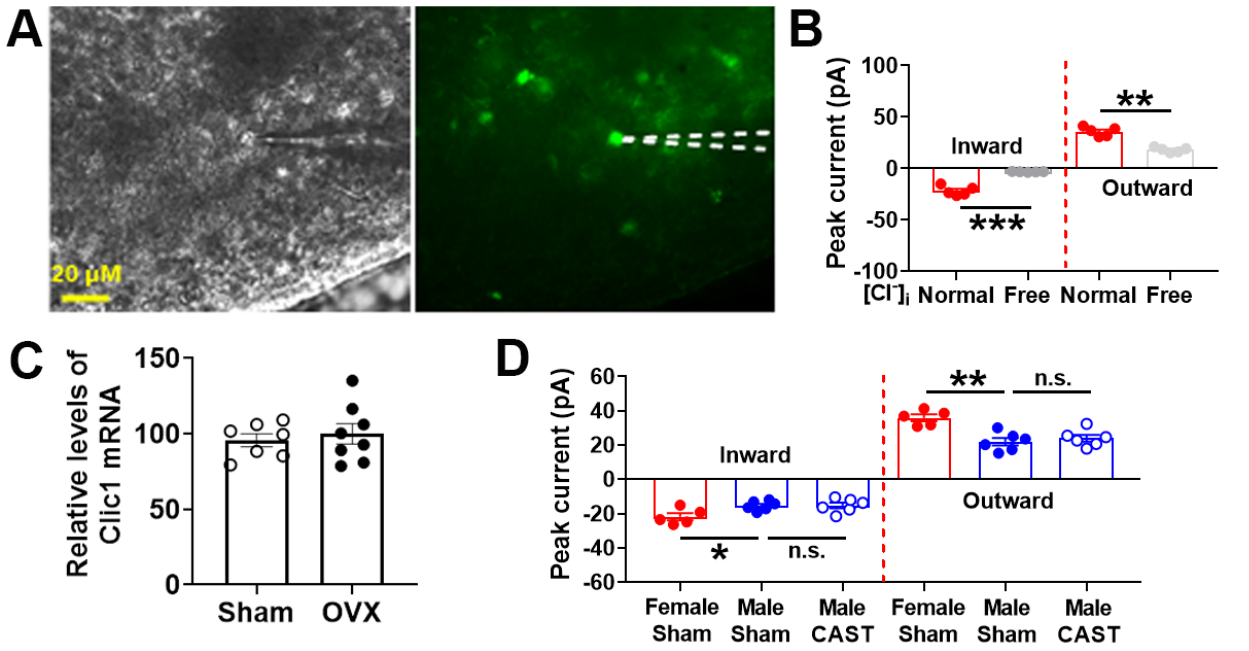

Figure S2. Clic1 currents in ERα^{vlVMH} neurons. (A) Representative bright field and green fluorescent microscopic images showing patch clamp recording of an ERα^{vlVMH} neuron in the brain slice from a female ERα-ZsGreen mouse. (B) Peak inward and outward IAA-94-senstive currents measured in ERα^{vlVMH} neurons with free intracellular [Cl^-]. Data are presented as mean ± SEM with individual data points. N =5 neurons from 3 different mice per group. **, P<0.01; ***, P < 0.001 in two-sided unpaired t-tests. (C) Relative levels of Clic1 mRNA in the mediobasal hypothalamus from sham or OVX female mice. Data are presented as mean ± SEM with individual data points. N =7 or 8 mice per group. (D) Peak inward and outward IAA-94-senstive currents measured in ERα^{vlVMH} neurons from sham female, sham male or castrated (CAST) male mice. Note that data from sham female group were the same as those presented in Figure 2B. Data are presented as mean ± SEM with individual data points. N =5 or 6 neurons from 3 different mice per group. *, P < 0.05; **, P < 0.01 in one-way ANOVA analysis followed by Tukey comparisons.

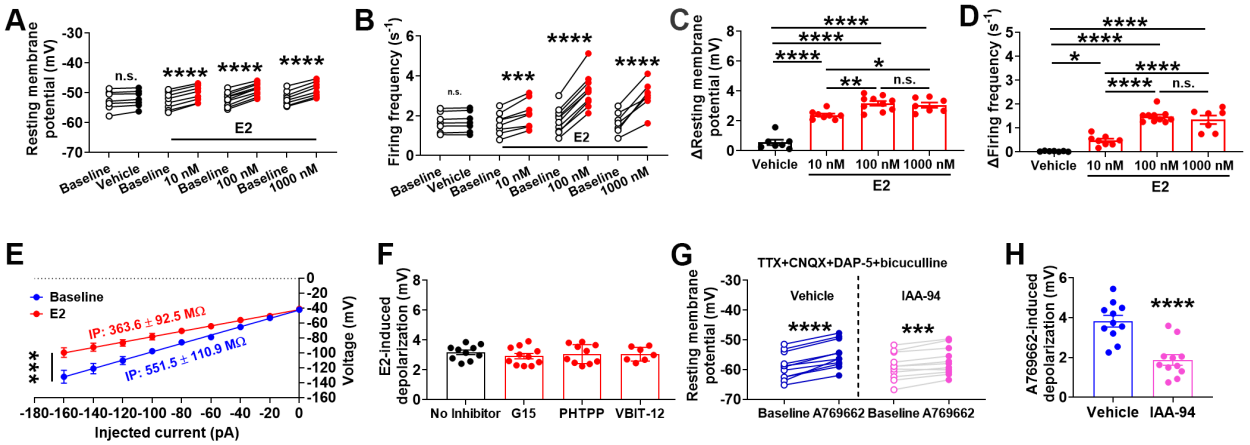

Figure S3. E2 activates ERα^{vlVMH} neurons. (A-B) Resting membrane potential (A) and firing frequency (B) of ERα^{vlVMH} neurons at the baseline and after E2 treatment (10, 100 or 1000 nM) 100 μM). Data are presented as individual data points. N =7, 8 or 10 neurons from 3 different mice per group. ***, P < 0.001; ****, P < 0.0001 in two-way ANOVA analysis followed by Sidak comparisons. (C-D) Changes in resting membrane potential (C) and firing frequency (D) calculated from (A-B) respectively. Data are presented as mean ± SEM with individual data points. N =7, 8 or 10 neurons from 3 different mice per group. *, P < 0.05; **, P < 0.01; ****, P < 0.0001 in one-way ANOVA analysis followed by Tukey comparisons. (E) I/V curves measured in ERα^{vlVMH} neurons at the baseline and after E2 treatment (100 nM) with input resistance (IP) calculated. Data are presented as mean ± SEM. N =6 neurons from 3 different mice per group. ***, P < 0.001in two-way ANOVA analysis. (F) Depolarization induced by 100 nM E2 in ERα^{vlVMH} neurons in the absence or presence of various inhibitors, including G15 (10 μM, a GPER inhibitor), PHTPP (50 μM, an ERβ inhibitor), and VBIT-12 (20 μM, a VDAC1 inhibitor). Data are presented as mean ± SEM with individual data points. N =10, 11 or 13 neurons from 3 different mice per group. (G) Resting membrane potential of ERα^{vlVMH} neurons at the baseline and after A769662 treatment (10 μM, an AMPK activator) in the presence or absence of IAA-94 (100 μM), with TTX (1 μM), CNQX (30 μM), D-AP5 (30 μM) and bicuculline (50 μM) in the perfusion buffer. Data are presented as individual data points. N =11 neurons from 3 different mice per group. ***, P < 0.001; ****, P < 0.0001 in two-way ANOVA analysis followed by Sidak comparisons. (H) Depolarization induced by 10 μM A769662 in ERα^{vlVMH} neurons in the absence or presence of IAA-94 (100 μM). N =11 neurons from 3 different mice per group. Data are presented as mean ± SEM with individual data points. ****, P < 0.0001 in two-sided unpaired t-tests.

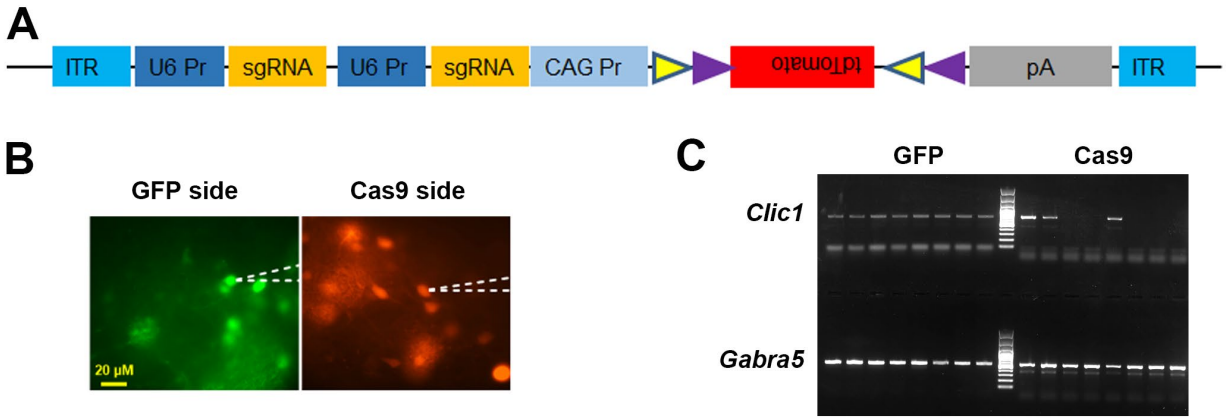

Figure S4. Cas9-mediated Clic1 disruption. (A) The schematic illustration of the AAV-Clic1/sgRNAs-FLEX-tdTOMATO construct. (B) Representative fluorescent microscopic images showing patch clamp recording of a control ERα^{vlVMH} neuron (GFP side) and an ERα^{vlVMH} neuron with Clic1 deleted (Cas9 side). (C) Two-step touchdown PCR detecting Clic1 and Gabra5 genomic sequences from single ERα^{vlVMH} neuron samples collected from the GFP or Cas9 side.

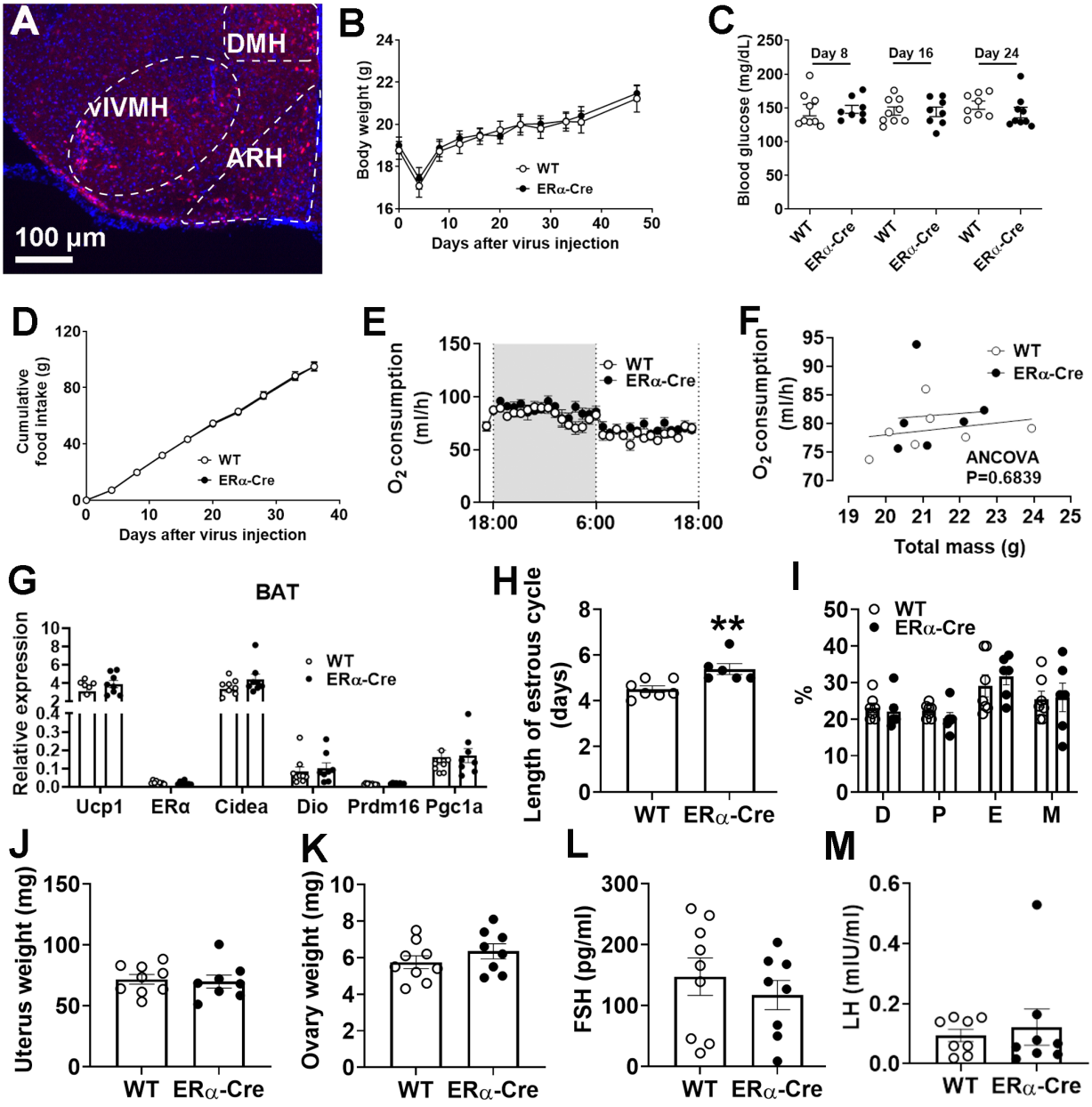

Figure S5. Phenotypes of chow-fed female mice lacking Clic1 in ERα^{vlVMH} and ERα^{ARH} neurons. (A) A representative microscopic image showing distribution of tdTomato (red) and DAPI (blue) in the mediobasal hypothalamus in ERα-Cre female mice receiving stereotaxic injections. ARH, arcuate nucleus of the hypothalamus; DMH, dorsomedial hypothalamus (DMH); vlVMH, ventrolateral subdivision of ventromedial hypothalamic nucleus. (B) Temporal changes in body weight in chow-fed WT and ERα-Cre female mice after stereotaxic injections of viruses. Data are presented as mean ± SEM. N =8 or 9 mice per group. (C) Blood glucose of chow-fed WT and ERα-Cre female mice measured at day 8, 16 and 24 after stereotaxic injections of viruses. Data are presented as mean ± SEM with individual data points. N =8 or 9 mice per group. (D) Cumulative food intake in chow-fed WT and ERα-Cre female mice after stereotaxic injections of viruses. Data are presented as mean ± SEM. N =8 or 9 mice per group. (E) O_2 consumption of

chow-fed WT and ERα-Cre female mice during the dark and light cycles. Data are presented as mean ± SEM. N =6 or 7 mice per group. (F) ANCOVA analysis of O_2 consumption with total body mass as a covariate. Data are presented as individual data points. N =6 or 7 mice per group. (G) Relative mRNA levels of indicated genes in BAT from chow-fed WT and ERα-Cre female mice. Data are presented as mean ± SEM with individual data points. N =8 or 9 mice per group. (H) Length of estrous cycle of chow-fed WT and ERα-Cre female mice. Data are presented as mean ± SEM with individual time points. N =6 or 7 mice per group. **, $P < 0.01$ in two-sided unpaired t-tests. (I) Length of diestrus (D), proestrus (P), estrus (E) and metestrus (M) as percentage of the estrous cycle of chow-fed WT and ERα-Cre female mice. Data are presented as mean ± SEM with individual time points. N =6 or 7 mice per group. (J-K) Weights of uterus (J) and ovaries (K) of chow-fed WT and ERα-Cre female mice. Data are presented as mean ± SEM with individual time points. N =8 or 9 mice per group. (L-M) Blood FSH (L) and LH (M) of chow-fed WT and ERα-Cre female mice. Data are presented as mean ± SEM with individual time points. N =8 or 9 mice per group.

Table S1. Protein candidates binding to ERα-WT by BioID-MS. Proteins candidates within the BioID-ERα group were selected based on a sum intensity threshold exceeding 20 times that of the control group (BioID group). These chosen proteins were considered as potential candidates for binding with ERα. Subsequently, all identified protein candidates from BioID-MS underwent further analysis using the David Bioinformatics database (https://david.ncifcrf.gov/summary.jsp). This analysis aimed to categorize membrane proteins based on their cellular component annotations within the database.